ESMO GOOD SCIENCE BETTER MEDICINE BEST PRACTICE

IOTECH IMMUNO-ONCOLOGY TECHNOLOGY

REVIEW

Molecular imaging for cancer immunotherapy

E. A. Lim[1*], C. G. Drake[1] & A. Mintz[2]

[1]Herbert Irving Comprehensive Cancer Center, Columbia University Irving Medical Center, New York; [2]Department of Radiology, Division of Nuclear Medicine, Columbia University Irving Medical Center, New York, USA

Available online 27 March 2020

Immunotherapy has changed the treatment landscape for many cancers; however, not all patients treated have a favorable response and others can develop immune-related adverse events. A method to predict the treatment response to immunotherapeutic agents could allow for improved selection of patients more likely to benefit from treatment while sparing those who would suffer serious complications. While this has been an active area of research and has resulted in significant insights, current proposed mechanisms do not fully explain responses to therapy. One problem is that our understanding relies mostly on tumor biopsy samples that do not account for the complex spatiotemporal heterogeneity of cancers and their microenvironment. Radiolabeled probes targeting immune biomarkers and imaged using positron emission tomography with computed tomography could provide *in vivo*, real-time and non-invasive imaging of these biomarkers. Here we review the current field of functional nuclear imaging agents in immuno-oncology including antibodies and small molecule tracers to image PD-1, PD-L1, CTLA-4, T-cell markers and other targets being studied for potential therapies.

Key words: immunotherapy, biomarker, PET, imaging

INTRODUCTION

Immunotherapy with the use of checkpoint inhibitors has transformed the treatment of cancers ranging from melanoma and non-small-cell lung cancer (NSCLC) to Hodgkin's lymphoma and Merkel cell carcinoma.[1] Along with these major advances, new questions and problems have arisen in this rapidly evolving area of medical oncology. In particular, while responses to these therapies can be seen in heavily pretreated patients and can be durable, they are also variable, ranging from 20% to 60%.[2,3] Furthermore, the kinetics of a tumor's response to immunotherapy can vary widely,[4] at times resulting in the premature discontinuation of an effective drug or the unnecessary continuation of an ineffective drug. Immunotherapy can also result in serious immune-related adverse events[5] and is associated with high costs.[6,7] These issues highlight the need to better understand which patients will respond to these novel treatments and which patients might suffer from increased toxicities. In addition to personalizing immunotherapy, having an objective quantifiable measure of response will expedite future development of immunotherapy and optimize combinatorial strategies.

A variety of biomarkers that predict tumor response to immunotherapy have been evaluated, including the expression levels of the programmed cell death protein 1 (PD-1) or its ligand (PD-L1),[8–12] the burden of tumor mutations and conditions resulting in increased neoantigen production,[13–15] the variations in T-cell signatures,[16] and the composition of flora within a patient's microbiome.[17,18] While these studies have added to our understanding of the field, they do not definitively predict or fully explain the disparate response of cancers to immunotherapy.

One issue limiting a more complete understanding of tumor biology and host interactions in the tumor microenvironment has been our reliance on tumor biopsies. A biopsy using an 18-gauge needle collects a tissue sample of 0.011cm^3, which may represent only 0.1% of a tumor.[19] This small snapshot may not accurately represent the heterogeneous expression of biomarkers within a tumor or across different metastatic sites.[20–24] The expression of PD-1, PD-L1 and other immune markers is also dynamic and depends on prior therapies.[25–27] Thus a single biopsy at a single time-point is likely insufficient, and repeat biopsies, with their associated complications, would be necessary to evaluate the complex spatiotemporal characteristics of tumors and their microenvironment.

Radiolabeled probes targeting immune biomarkers may help to overcome some of the challenges of tumor biopsies. These agents, imaged using single photon emission computed tomography (SPECT) or positron emission tomography with computed tomography (PET/CT), can

*Correspondence to: Dr Emerson A. Lim, Herbert Irving Comprehensive Cancer Center, Columbia University Irving Medical Center, 161 Fort Washington Avenue, 9th floor, New York, NY 10032, USA. Tel: 212 305-5874
E-mail: el2342@cumc.columbia.edu (E. A. Lim).

provide *in vivo*, real-time and non-invasive imaging of tumor biomarker expression and immune responses to novel therapies. In particular, PET/CT is a highly sensitive and quantitative imaging modality that can allow for evaluation of an entire tumor and its associated metastases, and can be repeated over serial time points to track tumor responses. Here, we review the current state of the art for functional nuclear imaging in immuno-oncology.

PD-1/PD-L1 ANTIBODIES

PD-1 is a transmembrane receptor found on T cells, B cells and natural killer (NK) cells. When bound to its ligand, PD-1 inhibits T-cell activation, inhibits apoptosis of tumor cells, and promotes effector T-cell exhaustion.[4,28] To date, the US Food and Drug Administration has approved six monoclonal antibodies blocking the PD-1/PD-L1 interaction. These agents include PD-1 inhibitors nivolumab, pembrolizumab and cemiplimab, and PD-L1 inhibitors atezolizumab, avelumab and duravlumab. Given the clinical success of PD-1 and PD-L1 inhibition for the treatment of advanced cancers, many radioligand imaging studies have targeted this receptor/ligand pair by radiolabeling PD-1 or PD-L1 antibodies.

Antibodies have relatively long circulating half-lives and often require several days to clear the background blood pool. As a result, the selection of the radioisotope to be conjugated to the antibody requires one with a comparable half-life. Indium-111 (^{111}In, $t_{1/2} = 67.3$ h) has been used in SPECT tracer studies,[27,29,30] while copper-64 (^{64}Cu, $t_{1/2} = 12.7$ h), iodine-124 (^{124}I, $t_{1/2} = 100.2$ h) and zirconium-89 (^{89}Zr, $t_{1/2} = 78.4$ h) have been studied more extensively for antibody labeling in PET tracer studies.[31] The spatial resolution and quantitation potential heavily favor the use of PET imaging over SPECT when feasible. Furthermore, the longer half-life, availability, stable radiochemistry and favorable dosimetry of ^{89}Zr make it ideal for radiolabeling antibodies with long plasma half-lives.

Using ^{111}In, Heskamp et al. radiolabeled PD-L1.3.1, a murine monoclonal IgG1 antibody directed against human PD-L1.[27] The radiotracer was studied in xenograft mouse models of human breast cancer cell lines expressing varying levels of PD-L1 implanted into female BALB/c nude mice. They found that the radiotracer only accumulated in tumors with high levels of PD-L1. Interestingly, they also saw a heterogeneous distribution of ^{111}In-PD-L1.3.1 on high-resolution imaging. The highest level of uptake was seen in the periphery of the tumors, which correlated with immunohistochemical findings. Josefsson et al. conducted a similar study but performed ^{111}In labeling of a murine PD-L1 antibody in an immune-intact mouse model of breast cancer.[30] Biodistribution of the PD-L1 antibody demonstrated uptake in tumors expressing PD-L1, but also in the spleen, liver, thymus, heart and lung. In order to block non-tumor binding, excess unlabeled antibody was administered and showed decreased uptake in the spleen with increased concentration in the tumor, suggesting that a pre-dosing strategy with unlabeled antibody could decrease non-specific uptake. The same group later radiolabeled atezolizumab with ^{111}In.[29] Immunodeficient mice were implanted with PD-L1-expressing ovarian, breast and lung cancer cell lines and corresponding negative controls. They similarly found specific and persistent high accumulation of the radiotracer in PD-L1-positive tumors but not in the negative controls. As atezolizumab is cross-reactive to human and mouse PD-L1, pre-dosing with unlabeled antibody was found to reduce non-specific uptake in the spleen.

Other groups have found similar results using ^{64}Cu- or ^{89}Zr-labeled PD-L1 antibodies for PET imaging studies in various mouse tumor models.[32–38] In these studies, tracer uptake was seen in PD-L1-expressing tumors and other organs including lymph nodes, salivary glands, spleen, liver and kidneys. Of note, Hettich et al. developed ^{64}Cu-labeled murine anti-PD-1 and anti-PD-L1 antibodies.[34] In addition to PD-L1 uptake in the spleen and lymph nodes, they also noted increased uptake in the lungs of wild-type mice compared with PD-L1-deficient mice. Treatment of these mice with interferon-γ (IFN-γ) resulted in a significant induction of PD-L1 expression in the lungs, which the investigators hypothesized might be why lung cancers tend to be more responsive to checkpoint inhibition and why pneumonitis can be an immune adverse reaction seen in patients receiving checkpoint inhibitors. They went on to create mouse models of melanoma cell lines, and treated them with radiation and antibodies against PD-L1 and cytotoxic T-lymphocyte-associated antigen-4 (CTLA-4). Five days after treatment, they found radiotracer uptake in tumors and their draining lymph nodes that corresponded to increased CD8+ T cells in treated mice. Using a Fab phage display library, Truillet et al. developed C4, an anti-PD-L1 antibody that is cross-reactive to both human and mouse PD-L1.[38] Labeling C4 with ^{89}Zr, they were able to detect PD-L1 expression in a patient-derived xenograft model created from a patient who responded durably to treatment with pembrolizumab and the CTLA-4 antibody, ipilumumab. In mouse xenograft models of lung cancer treated with vehicle, paclitaxel or doxorubicin, PET/CT imaging was also able to detect significantly higher levels of ^{89}Zr-C4 in tumors treated with paclitaxel compared with other arms; other groups have confirmed this phenomenon with immunohistochemistry.[39]

With the background of these initial small animal models, Cole et al. evaluated the biodistribution and clearance of ^{89}Zr-nivolumab in healthy non-human primates, finding the highest uptake in the spleen and liver; this could be blocked with co-administration of excess unlabeled nivolumab.[40] Bensch et al. went on to report the first in-human experience of ^{89}Zr-atezolizumab administration.[41] Twenty-two patients with locally advanced or metastatic bladder cancer, NSCLC or triple-negative breast cancer underwent PET/CT imaging with ^{89}Zr-atezolizumab prior to treatment with atezolizumab. Uptake of the radiotracer was noted in the bone marrow, spleen and tumors. Importantly, heterogeneity in uptake was observed intratumorally in large tumors as well as in different metastatic lesions in the same patient, supporting the notion of tumor biomarker heterogeneity and demonstrating the power of PET molecular imaging to visualize real-time biomarker expression. Furthermore, on a per-lesion level, the baseline uptake on

PD-L1 PET imaging was correlated with lesions demonstrating the best response to anti-PD-L1 immunotherapy. Compared with biopsy samples for PD-L1 IHC and RNA sequencing, ^{89}Zr-atezolizumab uptake was more strongly related to response, progression-free survival and overall survival. This demonstrates the power of PET molecular imaging to potentially personalize a patient's therapeutic regimen based on targeted biomarker expression.

PD-1/PD-L1 SMALL MOLECULES

While there are many advantages to radiolabeling antibodies for PET/CT imaging, there are also several limitations. As mentioned previously, antibodies have long circulating half-lives. This results in higher background-to-signal ratios that require optimally imaging several days after injection of the radiotracer, limiting clinical workflow. The long circulating half-lives also result in the need to use long-lived radioisotopes and longer radiation exposure to patients. The size of antibodies may also impede their diffusion into solid tissues where cells expressing PD-1 and PD-L1 might be found. Factors affecting antibody uptake include blood vessel density, vascular permeability, interstitial fluid pressures and tumor growth kinetics. These variations could make PET imaging with antibodies suboptimal.[29] Finally, antibodies contain Fc domains which can activate antibody-dependent cellular cytotoxicity, and — if binding to PD-1 on T cells — may actually deplete the T cells mediating the antitumor response.[42–45]

To address problems that have arisen from the use of antibodies, groups have developed lower molecular weight tracers.[46] These smaller imaging agents tend to be cleared more quickly by the kidneys, allowing for same-day imaging and use of radiotracers with shorter half-lives including gallium-68 (^{68}Ga, $t_{1/2}$ = 68 min) and fluorine-18 (^{18}F, $t_{1/2}$ = 109 min). A variety of lower molecular weight tracers have been developed, including simple single-chain variable fragments, which contain the variable regions expressed as a single fusion protein, and more complex designs that combine various regions of the immunoglobulin scaffolding with the antigen-binding domain, such as minibodies.[47–49] Other examples of smaller protein-based radiotracers include nanobodies, single-domain antigen binding fragments of camelid heavy chain antibodies;[50,51] affibody molecules, non-antibody protein scaffolds of three helical domains that can be modified for a specific target;[52,53] adnectins, proteins derived from the 10th type III domain of human fibronectin engineered to provide high binding affinity to targets;[54,55] and engineered proteins developed by custom designing[44] or directed evolution.[43,56]

Using directed evolution with yeast display, Maute et al. engineered a non-antibody biologic molecule based on the ectodomain of PD-1.[43] They produced a high-affinity consensus (HAC) molecule that bound to human PD-L1 with an equilibrium dissociation constant (K_D) of 100 pM. In murine models of colon cancer expressing PD-L1, they found that HAC was able to penetrate throughout the tumor, while anti-PD-L1 antibodies were found only at the peripheral and perivascular regions of the tumor, suggesting that HAC could bind to PD-L1 on tumor cells that were otherwise inaccessible to the antibody. While the 4-h incubation time of the anti-PD-L1 antibody in their mouse models may not have been long enough to allow for full penetration of the antibody into the tumor, co-treatment of PD-L1 antibody with CTLA-4 blockade saw no additional benefit, while the combination of CTLA-4 blockade with HAC resulted in smaller tumors. The investigators hypothesized that molecules penetrating more deeply into tumors might have improved efficacy. Labeling HAC with ^{64}Cu showed strong tumor-to-muscle and tumor-to-blood signal 1 h after injection, although it did also demonstrate high signal in the liver, consistent with copper-specific binding by liver proteins. The same group modified the radio-labeling of HAC by modifying the linker, glycosylation and the radiometal generating four molecules: ^{64}Cu-DOTA-HAC, ^{64}Cu-NOTA-HAC, ^{68}Ga-DOTA-HAC and ^{68}Ga-NOTA-HAC. They found that ^{64}Cu-NOTA-HAC most accurately visualized human PD-L1 expression in vivo, and that aglycosylation eliminated non-specific glandular uptake in the head and neck as well as decreased uptake in the spleen and liver.[57] This work indicates that modification of agents may optimize binding and imaging properties, and could potentially be used to improve imaging characteristics of other promising molecules.

Using adnectin-based technology, Donnelly et al. developed BMS-986192 directed against PD-L1.[54] Tagging it with ^{18}F, they were able to detect PD-L1-expressing tumors in mouse models. After non-human primate studies, the research group went on to perform first-in-human studies of ^{18}F-BMS-986192 and ^{89}Zr-nivolumab in 13 patients with advanced NSCLC prior to treatment with nivolumab.[58] They found that ^{18}F-BMS-986192 was able to find numerically more lesions, and that uptake in tumors was heterogeneous between and within patients. Uptake of ^{18}F-BMS-986192 correlated with tumor PD-L1 expression measured by immunohistochemistry, while uptake of ^{89}Zr-nivolumab correlated with PD-1-positive tumor-infiltrating cells. With their small sample size, they saw that there was higher (although not significant) uptake of ^{18}F-BMS-986192 in patients who responded to 3 months of nivolumab therapy compared with patients without a response peak standard uptake value (SUV_{peak}) 4.2 vs 2.2, P=0.89). On a per-lesion basis, uptake of ^{18}F-BMS-986192 was higher for responding lesions than non-responding lesions (SUV_{peak} 6.5 vs 3.2, P=0.03). Interestingly, there was slight uptake of ^{18}F-BMS-986192 in the hypophysis. While hypophysitis is an uncommon immune-related toxicity of immunotherapy, this finding may help to explain this phenomenon. Additional work to image larger populations of patients will be necessary to evaluate whether a certain threshold of radiotracer uptake in the hypophysis or other normal organs is associated with immune-related side-effects.

T-CELL TRACERS

While there has been significant interest in imaging the PD-1/PD-L1 axis, tracking the localization and kinetics of the

effector cells of the immune system has also been an area of active research.[59] Groups have pursued different strategies including targeting T-cell surface markers with PET radiotracers and targeting metabolic pathways upregulated in activated T cells.

Tavare et al. developed two ^{64}Cu-labeled minibody fragments against CD8.[47] These were injected into antigen-positive, antigen-negative, immunodeficient, antigen-blocked and antigen-depleted mice to evaluate specificity of uptake in lymphoid tissues. They found specific uptake in the spleen and lymph nodes of antigen-positive mice that was confirmed on *ex vivo* analysis. In order to improve imaging characteristics, the same group generated a ^{89}Zr-labeled anti-CD8 diabody, ^{89}Zr-malDFO-169.[49] They tested this agent in three preclinical mouse models treated with antigen-specific adoptive T-cell transfer, agonistic antibody therapy (anti-CD137) and checkpoint blockade (anti-PD-L1). The treated mice in each tumor model had increased radiotracer uptake compared with controls. Interestingly, in mice treated with the agonistic anti-CD137 antibody and mice treated with anti-PD-L1 antibody, responding mice had intratumoral uptake of the radiotracer while non-responders had only a peripheral rim of uptake. In a similar strategy, Rashidian et al. generated a ^{89}Zr-labeled PEGylated nanobody against CD8, ^{89}Zr-PEG-VHH-X118.[60] In mouse models of melanoma and breast cancer treated with CTLA-4 blockade, tumors that responded to therapy had homogeneous intratumoral uptake of the radiotracer, while those that did not respond had heterogenous uptake. This suggests that the pattern of radiotracer uptake may be an important characteristic in predicting treatment responses to immunotherapy. More recently, Pandit-Taskar et al.[61] used ^{89}Zr-Df-IAB22M2C, an anti-CD8 minibody, in a phase I dose escalation study to image six patients receiving or planning to receive immunotherapy. They found uptake of the radiotracer in the spleen, marrow and liver, as well as normal-appearing lymph nodes. While there was tumor uptake in metastatic lesions for patients with melanoma and hepatocellular carcinoma, four patients with lung metastases had no tracer uptake. As the study included patients with multiple tumor types at various points in treatment and no follow-up data, it is difficult to interpret these results. However, this study demonstrated feasibility and safety as well as a biodistribution of radiotracer consistent with CD8+ T-cell-enriched tissues.

Other groups have evaluated tracers targeting the more general T-cell marker, CD3. Evaluating a ^{89}Zr-labeled anti-CD3 antibody in syngeneic mouse tumor models, Beckford Vera et al. found increased uptake in tumors.[62] Interestingly, they saw that while they did not deplete CD8 T cells, the pool of naïve CD8 T cells was decreased and effector memory CD8 T cells increased, while the CD4 T cell pool was diminished. Larimer et al. evaluated another ^{89}Zr-labeled CD3 PET probe, ^{89}Zr-DFO-CD3, in a murine tumor model treated with anti-CTLA-4 therapy.[63] Increased tumor uptake was able to differentiate mice that would eventually have smaller tumors.

Another strategy to visualize T cells is to evaluate the dynamics of T-cell activation. While most cells utilize the *de novo* pathway for DNA synthesis, lymphoid cells rely heavily on the salvage pathway.[64] Understanding this underlying biology, Radu et al. identified 1-(2'-deoxy-2'-^{18}F fluoarabinofuranosyl) cytosine (^{18}F-FAC) by differential screening.[64] They found that ^{18}F-FAC was phosphorylated and trapped in lymphoid cells by deoxycytidine kinase (dCK). In a murine sarcoma model, they found that at the peak of antitumor immune response, ^{18}F-FAC PET showed increased accumulation in the spleen and draining lymph nodes compared with baseline. Further evaluation of the splenic CD8 T cells showed a four-fold uptake of ^{18}F-FAC in effector CD8+ T cells compared with naïve T cells. Using the same probe and magnetic resonance imaging (MRI) in a syngeneic mouse model of malignant glioblastoma, Antonios et al.[65] tracked mice treated with a dendritic cell vaccine with or without PD-1 blockade. They found that the ratio of contrast enhancement on MRI to normalized PET probe uptake (termed the 'immunotherapeutic response index') identified regions of immune activation, which they confirmed by enumeration of intracranial tumor infiltrating lymphocytes. They further saw a direct linear correlation between the immunotherapeutic response index and median survival (R^2=0.995).

As ^{18}F-FAC is rapidly catabolized by cytidine deaminase, it cannot be used as an imaging agent in humans. Kim et al.[66] found that 2-chloro-2'-deoxy-2'-^{18}F fluoro-9β-D-arabinofuranosyl-adenine (^{18}F-CFA) accumulated in tissues with high dCK expression in humans. Antonios et al. performed ^{18}F-CFA PET imaging on patients with recurrent glioblastoma before and after treatment with an autologous tumor lysate-pulsed dendritic cell vaccine and PD-1 blockade.[65] They found that in one evaluable patient imaged 3 weeks after treatment, there was^{18}F-CFA uptake in several peripheral lymph nodes and tumor compared with the baseline scan.

Roland et al. evaluated the use of 2'-deoxy-2'-^{18}F fluoro-9β-D-arabinofuranosyl-guanine,[67] which is phosphorylated by cytosolic dCK or mitochondrial deoxyguanosine kinase. Using this PET tracer in a mouse model of acute graft vs host disease (GVHD), they found that mice with acute GVHD had higher uptake in the cervical and mesenteric lymph nodes and spleen compared with controls.

OTHER TARGETS

Another way to evaluate the activation and function of CD8+ cytotoxic T cells in tumors is to measure the expression of intratumoral granzyme B or T-cell expression of OX-40. Granzyme B is a serine protease stored in the secretory granules of cytotoxic T lymphocytes and NK cells. On recognition of their target, T cells release granzyme which results in apoptosis in the target cell.[68] Larimer et al. developed a ^{68}Ga-labeled molecule, GZP, that irreversibly binds granzyme B.[19] In mouse models of colon cancer

treated with PD-1 blockade alone or PD-1 with CTLA-4 blockade, ^{68}Ga-GZP was able to detect intratumoral granzyme B and was able to differentiate treatment responders from treatment non-responders prior to divergence of tumor volume. Interestingly, granzyme B expression within an individual tumor was heterogeneous and did not correlate with number of CD8+ cells, suggesting that not all CD8+ T cells within a tumor are activated and a functional marker of activity may serve as a better way to predict treatment efficacy. A humanized molecule against granzyme B was also evaluated in on-treatment human melanoma specimens and correlated with responders versus non-responders. They went on to evaluate two murine colon cancer models treated with checkpoint inhibition, and saw that ^{68}Ga-GZP was able to predict response to immunotherapy with sensitivity of 93%, specificity of 87% and negative predictive power of 94%.[69] ^{68}Ga-GZP uptake was also noted to be linearly correlated with percent survival, suggesting that granzyme B can serve as an early biomarker for tumors responding to immunotherapy.

Part of the tumor necrosis factor (TNF) receptor superfamily, OX-40 is a type 1 transmembrane glycoprotein that acts as a co-stimulatory molecule on T cells.[70] On binding of the OX-40 ligand, found on activated antigen-presenting cells, TNF-receptor-associated factors are recruited, forming a T-cell-receptor-independent signaling complex. As a result, IL-2 and IFN-γ are secreted, which promotes the survival, proliferation and activation of T cells. It is thought that OX-40 expression is restricted to antigen-specific activated T cells. Alam et al. developed a ^{64}Cu-labeled murine OX-40 monoclonal antibody.[71] In a murine model, CpG oligonucleotide was administered into tumors as an intratumoral vaccine adjuvant. They saw increased uptake in injected tumors and draining lymph nodes as soon as 2 days after injection; however, 9 days after injection, signal was seen in the spleen. Interestingly, radiotracer uptake at the early imaging time point was able to predict responders from non-responders with 83% accuracy, 82% specificity and 85% sensitivity.

Blockade of CTLA-4 or CD152 with ipilimumab has also demonstrated efficacy in patients with metastatic melanoma and renal cell carcinoma.[72,73] Expressed on CD4+ regulatory cells, CD4+ effector cells and activated CD8+ effector cells, it competes with the T-cell co-stimulatory receptor CD28 for ligands CD80 and CD86 expressed on antigen-presenting cells. On activation, it is thought to downregulate the immune system.[74] A number of studies have evaluated the localization of CTLA-4 by PET. Using a ^{64}Cu-labeled anti-mouse CTLA-4 monoclonal antibody against the extracellular domain of CTLA-4, Higashikawa et al.[75] were able to show that CTLA-4 expression was present only in syngeneic immunocompetent mouse models of colon cancer. Others have evaluated the use of ^{64}Cu-ipilimumab and a ^{64}Cu-labeled fragment of ipilimumab lacking the Fc domain[76,77] in humanized mouse models. They demonstrated uptake in tumors expressing CTLA-4[76] and in salivary glands in a model of GVHD. Ingram et al.[78] used H11, a ^{89}Zr-labeled high-affinity alpaca heavy chain only antibody fragment that lacked an Fc portion targeting CTLA-4, to study the distribution of CTLA-4 in a B16 melanoma mouse model. They saw that CTLA-4 was mainly found in the tumor. Interestingly, they also noted that while H11 bound tightly to CTLA-4 and blocked the interaction with its ligands, it did not promote an antitumor response. Responses were seen when they modified the molecule to include a murine IgG2a constant region on H11. Responses were associated with regulatory T-cell depletion not seen in mice treated with H11, suggesting that CTLA-4 targeting requires Fc-dependent regulatory T-cell depletion.

PET imaging has also been used to evaluate the immunosuppressive signals within the tumor microenvironment. Indoleamine 2,3-dioxygenase (IDO) is an enzyme involved in the degradation of tryptophan to kynurenine. Depletion of tryptophan and accumulation of kynurenine and other downstream metabolites suppresses effector T-cell function and favors the differentiation of immunosuppressive regulatory T cells.[79] Increased expression of IDO is also associated with poorer survival, and use of IDO inhibitors is now being studied in clinical trials with varying success.[80,81] In order to image IDO, Huang et al. developed ^{18}F-IDO49, a radiofluorinated carboximidamide, and found that it specifically targeted IDO1 expressed in IFN-γ-expressing HeLa cells.[82] In mouse models of HeLa xenografts treated with or without IFN-γ, the team found increased uptake of ^{18}F-IDO49 in the tumors of mice treated with IFN-γ. The increased uptake of ^{18}F-IDO49 correlated with increased IDO1 expression by Western blot and immunohistochemistry.

Another immunosuppressive pathway is the generation of the purine nucleoside, adenosine, in the tumor microenvironment. It is generated by actions of the ectonucleotidases CD39 (which converts ATP to ADP and/or AMP) and CD73 (which dephosphorylates AMP to adenosine).[83] The suppressive effects of adenosine are mediated by the adenosine receptors, with A2AR being the most prevalent receptor across immune cells.[84,85] Activation of A2AR results in inhibition of effector T cells and NK cells,[86] and has led to a number of preclinical and clinical trials blocking this pathway by inhibiting the generation of adenosine or blocking A2AR. Interestingly, A2AR is also expressed in the brain, mostly in the caudate and putamen, and has also been an area of interest in neurology as it has been implicated in neurodegenerative diseases such as Alzheimer's dementia and schizophrenia.[87] While PET imaging of A2AR has not been studied in tumors, human studies have been performed to image A2AR in the brain. Barret et al. generated a fluorinated small molecule, ^{18}F-MNI-444, and were able to successfully image the healthy human brain.[87] They found uptake in the caudate and putamen, with low uptake in the cerebellum and cerebral cortex as expected. Whole-body PET scans of ^{18}F-MNI-444 were also performed in the same subjects and found excretion of the tracer via the hepatobiliary system but low uptake in other organs, suggesting this may be a promising tracer for oncology.

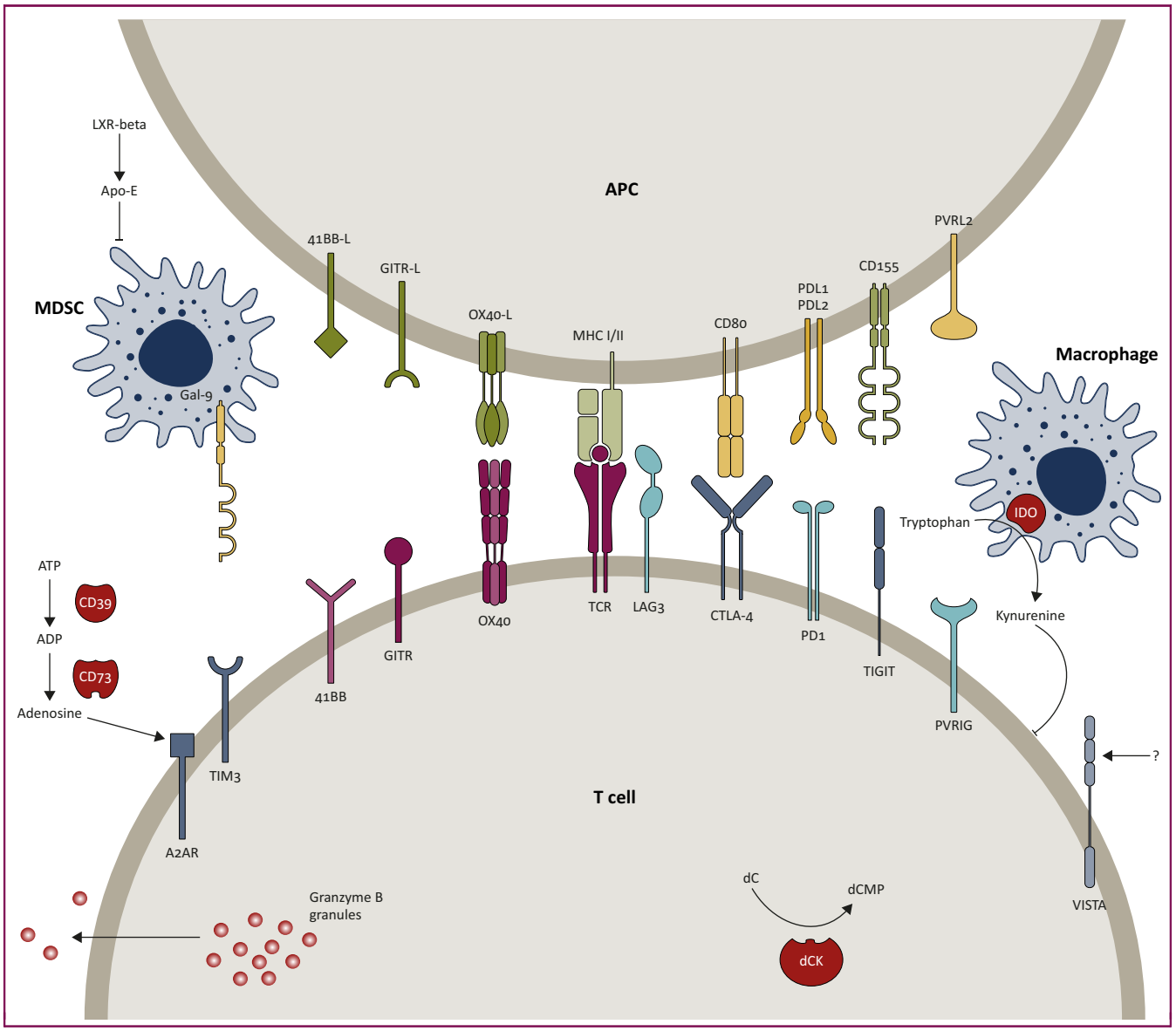

Figure 1. Potential targets for immunotherapy and immuno-positron emission tomography imaging.
Created with BioRender. 41BB-L, 41BB ligand; A2AR, adenosine A_{2A} receptor; ADP, adenosine diphosphate; APC, antigen-presenting cell; ATP, adenosine triphosphate; CTLA-4, cytotoxic T-lymphocyte-associated antigen-4; dCK, deoxycitidine kinase; dC, deoxycytidine; dCMP, deoxycitidine monophosphate; GITR, glucocorticoid-induced tumor necrosis factor receptor-related gene; IDO, indoleamine 2,3-dioxygenase; LAG3, lymphocyte activating gene 3; LXR-beta, liver x receptor beta; MDSC, myeloid-derived suppressor cell; MHC, major histocompatibility complex; PD1, programmed cell death protein 1; PDL1/L2, programmed cell death ligand 1/2; PVRIG, poliovirus-receptor-related immunoglobulin domain containing; PVRL2, poliovirus-receptor-related 2; TCR, T-cell receptor; TIGIT, T-cell immunoreceptor with Ig and ITIM domains; TIM3, T-cell immunoglobulin and mucin-domain containing-3; VISTA, V-domain immunoglobulin (Ig)-containing suppressor of T-cell activation.

Sakata et al. also performed PET imaging in healthy volunteers using ^{11}C-preladenant and found similar results;[88] however, with a half-life of 20 min, ^{11}C may be a more difficult radioisotope to use more widely.

FUTURE DIRECTIONS

In the future, immuno-PET imaging may be used as a biomarker to predict response to immunotherapy and help guide the care of cancer patients. A scan prior to initiating treatment could be used to determine whether a patient's tumor would respond well to a particular immunotherapy. It could also be used to see whether a patient might suffer more adverse effects from that therapy. Another potential application would be to track early responses to treatment. This could allow providers to switch therapies in patients not responding favorably, and thus avoid unnecessary side-effects and reduce costs associated with ineffective treatment. Immuno-PET may also improve our understanding of the immune microenvironment and the mechanisms of action of different immunotherapies, thereby providing a way to further investigate novel targets and optimize therapeutic strategies.

While the studies reviewed here lay a strong preclinical foundation and present promising preliminary first-in-human data, this novel imaging modality is still very much in development and more work is needed before it can be

Table 1. **Human studies for immuno-PET imaging in cancer.**

Clinicaltrials.gov identifier	Tracer	Tracer target	Patient population	Recrutiment site(s)/ manufacturer	*N*	Study details	Estimated completion date
NCT03802123	[^{89}Zr] Df-IAB22M2C	CD8	Metastatic solid tumors	CARTI Cancer Center, MSKCC/ ImaginAb Inc.	40	Imaging 1 week prior to and 4—5 weeks after starting cancer therapy. Correlation between [^{89}Zr]-Df-IAB22M2C uptake with immune infiltrates and other molecular biomarkers (CD4, CD8, PD-1 and PD-L1) expression by IHC on biopsy samples taken around the same timepoints	December 2019
NCT03313323	[^{89}Zr] ipilimumab	CTLA-4	Metastatic melanoma planned to get ipilumumab	VU University Medical Center/ BMS	29	[^{89}Zr] ipilimumab PET imaging 2 h after the first and second dose of ipilumumab	February 2020
NCT03506802	[^{18}F] FHBG	HSV-1 thymidine kinase gene	Recurrent or refractory multiple myeloma	UCLA Jonsson Comprehensive Cancer Center, National Cancer Institute, California Institute for Regenerative Medicine	12	Subjects will be treated with adoptive T-cell transfer with NY-ESO-1 TCR engineered peripheral blood mononuclear cells and peripheral blood stem cells. PET imaging will be performed to determine whether these cells home to the bone marrow, lymph nodes or extramedullary sites	May 2022
NCT03089606	[^{11}C] AMT	IDO	Metastatic melanoma treated with pembrolizumab	UNC Lineberger Comprehensive Cancer Center/ Merck	25	[^{18}F] FDG and [^{11}C] AMT PET imaging prior to standard pembrolizumab treatment; pre-treatment biopsies will be performed to correlate to imaging; AMT PET scan SUV levels will be correlated to overall response rate at 12 weeks after initiation of treatment	June 2022
NCT02922283	[^{18}F] FB-IL-2	IL2	Metastatic melanoma	University Medical Center Groningen	30	[^{18}F] FB-IL-2 PET at baseline and 6 weeks after therapy with ipilimumab, nivolumab, pembrolizumab or ipilimumab with nivolumab	August 2023
NCT03780725	[^{89}Zr] BI 754111	LAG3	NSCLC and SCCHN	VU Medisch Centrum, Netherlands/Boehringer Ingelheim	40	Subjects are treated with the BI 754111 (LAG3 mAb) and BI 754091 (PD-L1 mAb)	July 2020
NCT03065764	[^{89}Zr] pembrolizumab	PD-1	NSCLC	VU University/Merck Sharp and Dohme Corp.	10	Two [^{89}Zr] pembrolizumab PET scans: one with and one without a preceding 'cold' therapeutic dose of pembrolizumab. First three subjects will undergo scans 1, 72, and 120 h after radiotracer injection	December 2019
NCT03520634	[^{18}F] PD-L1	PD-L1	Metastatic melanoma treated with PD-L1 therapy	University Medical Center Groningen	15	[^{18}F] PD-L1 scan at baseline and 6 weeks after therapy with paired biopsies if feasible	October 2023
NCT02453984	[^{89}Zr] atezolizumab	PD-L1	Locally advanced or metastatic tumors	University Medical Center Groningen	54	Fresh pre-treatment and [^{89}Zr] atezolizumab PET scan to be correlated	September 2022
NCT03850028	[^{89}Zr] atezolizumab	PD-L1	DLBCL	VU University Medical Center, University Medical Center Groningen, Stichting Hemato-Oncologie voor Volwassenen Nederland/Hoffman-La Roche	20	[^{89}Zr] atezolizumab PET at baseline and after induction with R-CHOP; subjects will then get atzolizumab consolidation; re-image at suspected progression	April 2025
NCT03746704	[^{89}Zr] DFO-REGN3504	PD-L1	Advanced thoracic malignancies, gastric cancer and gastroesophageal junction adenocarcinoma	Regeneron	28	To establish an adequate mass dose and activity dose of [^{89}Zr] DFO-RGFN3504 and to establish test/ re-test reliability on two separate imaging time points	June 2021
NCT03829007	[^{89}Zr] durvalumab	PD-L1	SCCHN	Radboud University, University Medical Center Groningen/ AstraZeneca	58	[^{89}Zr] durvalumab imaging prior to treatment with durvalumab 1500 mg every 4 weeks; correlation with PD-L1 expression performed by Ventana SP263 antibody	March 2021
NCT03853187	[^{89}Zr] durvalumab	PD-L1	NSCLC	Radboud University/ AstraZeneca	20	[^{89}Zr] durvalumab imaging prior to two doses of neoadjuvant durvalumab followed by curative	April 2022

Continued

Table 1. Continued

Clinicaltrials.gov identifier	Tracer	Tracer target	Patient population	Recrutiment site(s)/ manufacturer	*N*	Study details	Estimated completion date
						surgery; 48 h prior to surgery injection of *ex vivo* In-111-oxine labelled autologous CD8+ T cells will be formed and scan on the day of surgery	
NCT03638804	[^{89}Zr] KN-035	PD-L1	Advanced PD-L1-expressing solid tumors	The First Affiliated Hospital of Soochow University/MITRO Biotech Co., Ltd.	10	To evaluate the biodistribution and target lesion uptake of [^{89}Zr] KN035 in patients with PD-L1-positive advanced solid tumors using PET imaging	December 2019
NCT03409419	[^{18}F] clofarabine	T-cell activation	Metastatic melanoma with progression of disease on PD-1/ PD-L1 therapy	UCLA Jonsson Comprehensive Cancer Center, National Cancer Institute/Tesaro Inc	10	[^{18}F clofarabine PET before and 2−4 weeks after treatment with TIM3 +/− PD-L1 therapy	August 2021
NCT03007719	[^{18}F] F-AraG	T-cell activation	Bladder cancer to receive atezolizumab in the neoadjuvant setting as part of a clinical trial or other immunotherapy as standard of care	UCSF/CellSight Technologies	31	Cohort 1: [^{18}F] F-AraG PET/MRI prior to neoadjuvant atezolizumab then prior to surgery. Cohort 2: [^{18}F] F-AraG PET/MRI before standard immunotherapy and on cycle 1 day 15 and cycle 2 day 7 of treatment	December 2019
NCT03129061	[^{18}F] F-AraG	T-cell activation	SCCHN	Stanford University/CellSight Technologies	24	Cohort 1: unresectable SCCHN treated with pembrolizumab imaged at baseline then 6−12 weeks after dose. Cohort 2: neoadjuvant pembrolizumab with imaging at baseline and 2−3 weeks after dose	June 2019
NCT03142204	[^{18}F] F-AraG	T-cell activation	Patients getting radiation therapy or immunotherapy	UCSF/CellSight Technologies	30	[^{18}F]F-AraG PET at baseline and after start of treatment	May 2021
NCT03311672	[^{18}F] F-AraG	T-cell activation	NSCLC	UCSF/CellSight Technologies	20	[^{18}F]F-AraG PET in patients receiving immunotherapy alone or with radiation. The correlation between number of infiltrating CD3+ T cells/μm^2 in the NSCLC thoracotomy specimen as quantified by IHC and the activated T-cell concentration as determined by [^{18}F]F-AraG PET (SUV_{max})	December 2020

A search performed on Clinicaltrials.gov using search terms 'cancer' and 'PET' that were not yet recruiting, recruiting, and active not recruiting yielded 1300 studies. Trials targeting immune mechanisms in cancer were selected from this larger list. 18F-AraG, 2'-deoxy-2'-^{18}F fluoro-9β-D-arabinofuranosyl-guanine; AMT, alpha-methyltryptophan; BMS, Bristol-Myers Squibb; CTLA-4, cytotoxic T-lymphocyte-associated antigen-4; DLBCL, diffuse large B-cell lymphoma; FDG, fluorodeoxyglucose; [^{18}F]FHBG, 9-(4-(18)F-Fluoro-3-[hydroxymethyl]butyl)guanine; HSV-1, herpes simplex virus type 1; IDO, indoleamine 2,3-dioxygenase; IHC, immunohistochemistry; IL-2, interleukin-2; MRI, magnetic resonance imaging; MSKCC, Memorial Sloan Kettering Cancer Center; NSCLC, non-small-cell lung cancer; PD-1, programmed cell death protein-1; PD-L1, programmed cell death ligand-1; PET, positron emission tomography; R-CHOP, rituxumab, cyclophosphamide, doxorubicin, vincristine, prednisone; SCCHN, squamous cell cancer of the head and neck; SUV, standard uptake value; TCR, T-cell receptor; UCLA, University of California, Los Angeles; UCSF, University of California, San Francisco; VU, Vrije Universiteit.

https://doi.org/10.1016/j.iotech.2020.03.001

used for these purposes. For example, it is unclear which aspects of these scans will be crucial to determine prognosis or predict treatment response. A lesion's baseline radiotracer uptake, determined by SUV, appears to be one measure that correlates with treatment response. A change in the SUV after starting treatment appears to be another candidate. Other imaging characteristics seen in the studies reviewed include the quality or distribution of radiotracer uptake: peripheral, heterogenous or homogenous. These elements are more qualitative, and further work will be needed to define these patterns for standardized quantitation and to see whether they correlate with outcome. All these factors are further complicated in patients with multiple metastases, as each metastatic site might have a different SUV or pattern of uptake. Further work will be needed to determine how to account for each lesion and its imaging characteristics. As other immunotherapeutic pathways and mechanisms are discovered, additional radiotracers will likely be evaluated. Targets currently being examined in preclinical or clinical studies include LAG-3,[89] TIM-3,[90] GITR,[91] TIGIT,[92] PVRIG,[93] SLAMF7,[94] VISTA,[95] LXR[96] and 4-1BB (See Figure 1 for potential immune targets. See Table 1 for ongoing human trials evaluating immuno-PET in cancer).[97] Other immunotherapeutic approaches include the use of personalized cancer vaccines, adoptive T-cell transfer, oncolytic viruses and T-cell-redirecting molecules. Predicting how any or all of these therapies will work for a particular patient will continue to be a challenge, and further studies validating predictive biomarkers will need to be done.

Spatial resolution is poor in PET imaging; however, the combination with CT allows for improved anatomic localization of radiotracer uptake. An approach that could improve information obtained from immuno-PET scans is to combine it with a different imaging modality such as MRI. Additional biologic and structural information obtained from PET/MRI may have more diagnostic and predictive abilities,[98] as has been seen in other areas such as infectious diseases,[99,100] neurology[101] and prostate cancer imaging.[102,103]

Radiomics, the use of quantitative features from standard imaging modalities to characterize tumor phenotype,[100] is another tool that could be combined with immuno-PET to provide additional information regarding the underlying characteristics of a cancer. Using radiomics, Aerts et al. were able to predict tumor epiderminal growth factor receptor mutation status in patients with early-stage NSCLC treated with neoadjuvant gefitinib.[104] Similarly, a radiomics signature developed by Sun et al. was able to identify inflamed tumours from non-inflamed tumors in a heterogeneous cohort of patients.[105] Those with an inflamed radiomics signature were more likely to have an objective response and had improved overall survival compared with those with a non-inflamed signature.

An extension of radiomics is the application of artificial intelligence (AI) and deep learning to imaging technologies. It offers the promise of enhancing the ability of clinicians to characterize and properly categorize lesions seen on scans in a uniform, robust and automated fashion.[106] Computer-aided detection and diagnosis has been shown to enhance the detection of lung cancers on low-dose chest CT, improve the identification of brain metastases on MRI, locate microcalcifications on screening mammography, and diagnose prostate lesions on multiparametric MRI.[106] Applying AI to immuno-PET scans may provide a more uniform, quantifiable and repeatable measure, and may be particularly helpful to evaluate patients who have numerous metastatic lesions. AI using radiomics has the potential to improve the standard measurements established by the Response Evaluation Criteria in Solid Tumors and World Health Organization, and its application to immuno-PET may provide a powerful new predictive and prognostic tool in oncology.

CONCLUSION

Immunotherapy has undoubtedly changed the landscape of cancer treatment; however, predicting which patients will benefit and which patients will suffer complications of therapy continues to be a challenge. Current predictive biomarkers such as PD-L1 status, tumor mutational burden and T-cell signatures have demonstrated some predictive ability; however, they are imperfect tests. One issue may be that these biomarkers are determined from tumor biopsies, which do not account for tumor heterogeneity within a single lesion and between metastatic sites. Radiographic evaluation using radioligands to identify biomarkers on PET/CT may help to solve this problem, as PET/CT is sensitive, quantitative and can be performed serially.

In this newly developing field of immuno-PET imaging, preclinical studies demonstrate promise, particularly with the use of PD-1- and PD-L1-directed radiolabeled antibodies and small molecules. Some of these radiotracers are now being tested in the clinic and again demonstrate encouraging results. However, as the context of expression of biomarkers within the tumor microenvironment will likely be important in providing a more complete picture of tumors and their behaviors, other markers are also being identified and imaged using PET/CT. These include T-cell markers as well as indicators of immune activation or suppression.

As additional immune pathways and targets are identified for cancer therapy, there will likely be additional radiotracers to image them. Paired with other standard imaging modalities such as MRI and coupled with the promise of radomics and AI, immuno-PET has the exciting potential to be a powerful tool that can provide revolutionary insights to cancer biology.

FUNDING

None declared.

DISCLOSURE

Dr Lim traveled to an investigator meeting for Bristol-Myers Squibb (BMS). Travel/lodging/meals were covered by the company; he holds stock options in Pfizer. Dr Drake has

undertaken consulting for AZ Medimmune, BMS, F-Star, Genocea, Janssen, Merck, Pierre Fabre, Roche/Genentech, Sanofi Aventis and EMD Serono; patents (held by Johns Hopkins University) for BMS and AZ Medimmune; and holds stock options in Compugen, Harpoon, Kleo, Shattuck Labs, Tizona and Werewolf. Dr Mintz serves as a paid consultant for Regeneron Pharmaceuticals Table 1.

REFERENCES

1. Hargadon KM, Johnson CE, Williams CJ. Immune checkpoint blockade therapy for cancer: an overview of FDA-approved immune checkpoint inhibitors. *Int Immunopharmacol*. 2018;62:29—39.
2. Carretero-Gonzalez A, Lora D, Ghanem I, et al. Analysis of response rate with ANTI PD1/PD-L1 monoclonal antibodies in advanced solid tumors: a meta-analysis of randomized clinical trials. *Oncotarget*. 2018;9:8706—8715.
3. Shields BD, Mahmoud F, Taylor EM, et al. Indicators of responsiveness to immune checkpoint inhibitors. *Sci Rep*. 2017;7:807.
4. Postow MA, Callahan MK, Wolchok JD. Immune checkpoint blockade in cancer therapy. *J Clin Oncol*. 2015;33:1974—1982.
5. Haanen J, Carbonnel F, Robert C, et al. Management of toxicities from immunotherapy: ESMO Clinical Practice Guidelines for diagnosis, treatment and follow-up. *Ann Oncol*. 2017;28:iv119—iv142.
6. Geynisman DM, Chien CR, Smieliauskas F, Shen C, Shih YC. Economic evaluation of therapeutic cancer vaccines and immunotherapy: a systematic review. *Hum Vacc Immunother*. 2014;10:3415—3424.
7. Aguiar Jr PN, Perry LA, Penny-Dimri J, et al. The effect of PD-L1 testing on the cost-effectiveness and economic impact of immune checkpoint inhibitors for the second-line treatment of NSCLC. *Ann Oncol*. 2017;28:2256—2263.
8. Shen X, Zhao B. Efficacy of PD-1 or PD-L1 inhibitors and PD-L1 expression status in cancer: meta-analysis. *BMJ*. 2018;362:k3529.
9. Balar AV, Galsky MD, Rosenberg JE, et al. Atezolizumab as first-line treatment in cisplatin-ineligible patients with locally advanced and metastatic urothelial carcinoma: a single-arm, multicentre, phase 2 trial. *Lancet*. 2017;389:67—76.
10. Rosenberg JE, Hoffman-Censits J, Powles T, et al. Atezolizumab in patients with locally advanced and metastatic urothelial carcinoma who have progressed following treatment with platinum-based chemotherapy: a single-arm, multicentre, phase 2 trial. *Lancet*. 2016;387:1909—1920.
11. Hirsch FR, McElhinny A, Stanforth D, et al. PD-L1 immunohistochemistry assays for lung cancer: results from phase 1 of the Blueprint PD-L1 IHC Assay Comparison Project. *J Thorac Oncol*. 2017;12:208—222.
12. Rehman JA, Han G, Carvajal-Hausdorf DE, et al. Quantitative and pathologist-read comparison of the heterogeneity of programmed death-ligand 1 (PD-L1) expression in non-small cell lung cancer. *Mod Pathol*. 2017;30:340—349.
13. Rizvi NA, Hellmann MD, Snyder A, et al. Cancer immunology. Mutational landscape determines sensitivity to PD-1 blockade in non-small cell lung cancer. *Science*. 2015;348:124—128.
14. McGranahan N, Furness AJ, Rosenthal R, et al. Clonal neoantigens elicit T cell immunoreactivity and sensitivity to immune checkpoint blockade. *Science*. 2016;351:1463—1469.
15. Le DT, Durham JN, Smith KN, et al. Mismatch repair deficiency predicts response of solid tumors to PD-1 blockade. *Science*. 2017;357:409—413.
16. Jiang P, Gu S, Pan D, et al. Signatures of T cell dysfunction and exclusion predict cancer immunotherapy response. *Nat Med*. 2018;24:1550—1558.
17. Liu K, Lu C. Gut microbes modulate host response to immune checkpoint inhibitor cancer immunotherapy. *Translat Cancer Res*. 2018;7:S608—S610.
18. Routy B, Le Chatelier E, Derosa L, et al. Gut microbiome influences efficacy of PD-1-based immunotherapy against epithelial tumors. *Science*. 2018;359:91—97.
19. Larimer BM, Wehrenberg-Klee E, Dubois F, et al. Granzyme B PET imaging as a predictive biomarker of immunotherapy response. *Cancer Res*. 2017;77:2318—2327.
20. Gerlinger M, Rowan AJ, Horswell S, et al. Intratumor heterogeneity and branched evolution revealed by multiregion sequencing. *N Engl J Med*. 2012;366:883—892.
21. Dill EA, Gru AA, Atkins KA, et al. PD-L1 expression and intratumoral heterogeneity across breast cancer subtypes and stages: an assessment of 245 primary and 40 metastatic tumors. *Am J Surg Pathol*. 2017;41:334—342.
22. Madore J, Vilain RE, Menzies AM, et al. PD-L1 expression in melanoma shows marked heterogeneity within and between patients: implications for anti-PD-1/PD-L1 clinical trials. *Pigment Cell Melanoma Res*. 2015;28:245—253.
23. McLaughlin J, Han G, Schalper KA, et al. Quantitative assessment of the heterogeneity of PD-L1 expression in non-small-cell lung cancer. *JAMA Oncol*. 2016;2:46—54.
24. Munari E, Zamboni G, Marconi M, et al. PD-L1 expression heterogeneity in non-small cell lung cancer: evaluation of small biopsies reliability. *Oncotarget*. 2017;8:90123—90131.
25. Zhang L, Wang J, Wei F, et al. Profiling the dynamic expression of checkpoint molecules on cytokine-induced killer cells from non-small-cell lung cancer patients. *Oncotarget*. 2016;7:43604—43615.
26. Rojko L, Reiniger L, Teglasi V, et al. Chemotherapy treatment is associated with altered PD-L1 expression in lung cancer patients. *J Cancer Res Clin Oncol*. 2018;144:1219—1226.
27. Heskamp S, Hobo W, Molkenboer-Kuenen JD, et al. Noninvasive imaging of tumor PD-L1 expression using radiolabeled anti-PD-L1 antibodies. *Cancer Res*. 2015;75:2928—2936.
28. Sharpe AH, Pauken KE. The diverse functions of the PD1 inhibitory pathway. *Nat Rev Immunol*. 2018;18:153—167.
29. Chatterjee S, Lesniak WG, Gabrielson M, et al. A humanized antibody for imaging immune checkpoint ligand PD-L1 expression in tumors. *Oncotarget*. 2016;7:10215—10227.
30. Josefsson A, Nedrow JR, Park S, et al. Imaging, biodistribution, and dosimetry of radionuclide-labeled PD-L1 antibody in an immunocompetent mouse model of breast cancer. *Cancer Res*. 2016;76:472—479.
31. Marciscano AE, Thorek DLJ. Role of noninvasive molecular imaging in determining response. *Adv Radiat Oncol*. 2018;3:534—547.
32. England CG, Ehlerding EB, Hernandez R, et al. Preclinical pharmacokinetics and biodistribution studies of 89Zr-labeled pembrolizumab. *J Nucl Med*. 2017;58:162—168.
33. England CG, Jiang D, Ehlerding EB, et al. (89)Zr-labeled nivolumab for imaging of T-cell infiltration in a humanized murine model of lung cancer. *Eur J Nucl Med Molec Imag*. 2018;45:110—120.
34. Hettich M, Braun F, Bartholoma MD, Schirmbeck R, Niedermann G. High-resolution PET imaging with therapeutic antibody-based PD-1/PD-L1 checkpoint tracers. *Theranostics*. 2016;6:1629—1640.
35. Lesniak WG, Chatterjee S, Gabrielson M, et al. PD-L1 detection in tumors using [(64)Cu]atezolizumab with PET. *Bioconjug Chem*. 2016;27:2103—2110.
36. Natarajan A, Mayer AT, Xu L, Reeves RE, Gano J, Gambhir SS. Novel radiotracer for immunoPET imaging of PD-1 checkpoint expression on tumor infiltrating lymphocytes. *Bioconjug Chem*. 2015;26:2062—2069.
37. Natarajan A, Patel CB, Habte F, Gambhir SS. Dosimetry prediction for clinical translation of (64)Cu-pembrolizumab immunoPET targeting human PD-1 expression. *Sci Rep*. 2018;8:633.
38. Truillet C, Oh HLJ, Yeo SP, et al. Imaging PD-L1 expression with immunoPET. *Bioconjug Chem*. 2018;29:96—103.
39. Luo M, Fu L. The effect of chemotherapy on programmed cell death 1/programmed cell death 1 ligand axis: some chemotherapeutical drugs may finally work through immune response. *Oncotarget*. 2016;7:29794—29803.
40. Cole EL, Kim J, Donnelly DJ, et al. Radiosynthesis and preclinical PET evaluation of (89)Zr-nivolumab (BMS-936558) in healthy non-human primates. *Bioorg Med Chem*. 2017;25:5407—5414.
41. Bensch F, van der Veen EL, Lub-de Hooge MN, et al. (89)Zr-atezolizumab imaging as a non-invasive approach to assess clinical response to PD-L1 blockade in cancer. *Nat Med*. 2018;24:1852—1858.

42. Brahmer JR, Drake CG, Wollner I, et al. Phase I study of single-agent anti-programmed death-1 (MDX-1106) in refractory solid tumors: safety, clinical activity, pharmacodynamics, and immunologic correlates. *J Clin Oncol*. 2010;28:3167—3175.
43. Maute RL, Gordon SR, Mayer AT, et al. Engineering high-affinity PD-1 variants for optimized immunotherapy and immuno-PET imaging. *Proc Natl Acad Sci U S A*. 2015;112:E6506—E6514.
44. Chatterjee S, Lesniak WG, Miller MS, et al. Rapid PD-L1 detection in tumors with PET using a highly specific peptide. *Biochem Biophys Res Commun*. 2017;483:258—263.
45. Broos K, Lecocq Q, Raes G, Devoogdt N, Keyaerts M, Breckpot K. Noninvasive imaging of the PD-1:PD-L1 immune checkpoint: embracing nuclear medicine for the benefit of personalized immunotherapy. *Theranostics*. 2018;8:3559—3570.
46. Nguyen V, Mintz A. New frontiers in biomarker-targeted molecular imaging. *Cancer Biol Ther*. 2009;8:2248—2251.
47. Tavare R, McCracken MN, Zettlitz KA, et al. Engineered antibody fragments for immuno-PET imaging of endogenous CD8+ T cells in vivo. *Proc Natl Acad Sci U S A*. 2014;111:1108—1113.
48. Olafsen T, Wu AM. Antibody vectors for imaging. *Semin Nucl Med*. 2010;40:167—181.
49. Tavare R, Escuin-Ordinas H, Mok S, et al. An effective immuno-PET imaging method to monitor CD8-dependent responses to immunotherapy. *Cancer Res*. 2016;76:73—82.
50. Broos K, Keyaerts M, Lecocq Q, et al. Non-invasive assessment of murine PD-L1 levels in syngeneic tumor models by nuclear imaging with nanobody tracers. *Oncotarget*. 2017;8:41932—41946.
51. De Meyer T, Muyldermans S, Depicker A. Nanobody-based products as research and diagnostic tools. *Trends Biotechnol*. 2014;32:263—270.
52. Frejd FY, Kim KT. Affibody molecules as engineered protein drugs. *Exper Molec Med*. 2017;49:e306.
53. Gonzalez Trotter DE, Meng X, McQuade P, et al. In vivo imaging of the programmed death ligand 1 by (18)F PET. *J Nucl Med*. 2017;58:1852—1857.
54. Donnelly DJ, Smith RA, Morin P, et al. Synthesis and biologic evaluation of a novel (18)F-labeled adnectin as a PET radioligand for imaging PD-L1 expression. *J Nucl Med*. 2018;59:529—535.
55. Sachdev E, Gong J, Rimel B, Mita M. Adnectin-targeted inhibitors: rationale and results. *Curr Oncol Rep*. 2015;17:35.
56. Nguyen V, Conyers JM, Zhu D, et al. A novel ligand delivery system to non-invasively visualize and therapeutically exploit the IL13Ralpha2 tumor-restricted biomarker. *Neuro Oncol*. 2012;14:1239—1253.
57. Mayer AT, Natarajan A, Gordon SR, et al. Practical immuno-PET radiotracer design considerations for human immune checkpoint imaging. *J Nucl Med*. 2017;58:538—546.
58. Niemeijer AN, Leung D, Huisman MC, et al. Whole body PD-1 and PD-L1 positron emission tomography in patients with non-small-cell lung cancer. *Nat Commun*. 2018;9:4664.
59. Griessinger CM, Maurer A, Kesenheimer C, et al. 64Cu antibody-targeting of the T-cell receptor and subsequent internalization enables in vivo tracking of lymphocytes by PET. *Proc Natl Acad Sci U S A*. 2015;112:1161—1166.
60. Rashidian M, Ingram JR, Dougan M, et al. Predicting the response to CTLA-4 blockade by longitudinal noninvasive monitoring of CD8 T cells. *J Exper Med*. 2017;214:2243—2255.
61. Pandit-Taskar N, Postow M, Hellmann M, et al. First-in-human imaging with (89)Zr-Df-IAB22M2C anti-CD8 minibody in patients with solid malignancies: preliminary pharmacokinetics, biodistribution, and lesion targeting. *J Nucl Med*. 2020;61:512—519.
62. Beckford Vera DR, Smith CC, Bixby LM, et al. Immuno-PET imaging of tumor-infiltrating lymphocytes using zirconium-89 radiolabeled anti-CD3 antibody in immune-competent mice bearing syngeneic tumors. *PLoS One*. 2018;13:e0193832.
63. Larimer BM, Wehrenberg-Klee E, Caraballo A, Mahmood U. Quantitative CD3 PET imaging predicts tumor growth response to anti-CTLA-4 therapy. *J Nucl Med*. 2016;57:1607—1611.
64. Radu CG, Shu CJ, Nair-Gill E, et al. Molecular imaging of lymphoid organs and immune activation by positron emission tomography with a new [18F]-labeled 2'-deoxycytidine analog. *Nat Med*. 2008;14:783—788.
65. Antonios JP, Soto H, Everson RG, et al. Detection of immune responses after immunotherapy in glioblastoma using PET and MRI. *Proc Natl Acad Sci USA*. 2017;114:10220—10225.
66. Kim W, Le TM, Wei L, et al. [18F]CFA as a clinically translatable probe for PET imaging of deoxycytidine kinase activity. *Proc Natl Acad Sci USA*. 2016;113:4027—4032.
67. Ronald JA, Kim BS, Gowrishankar G, et al. A PET imaging strategy to visualize activated t cells in acute graft-versus-host disease elicited by allogenic hematopoietic cell transplant. *Cancer Res*. 2017;77:2893—2902.
68. Rousalova I, Krepela E. Granzyme B-induced apoptosis in cancer cells and its regulation (review). *Int J Oncol*. 2010;37:1361—1378.
69. Larimer BM, Bloch E, Nesti S, et al. The effectiveness of checkpoint inhibitor combinations and administration timing can be measured by granzyme B PET imaging. *Clin Cancer Res*. 2019;25:1196—1205.
70. Willoughby J, Griffiths J, Tews I, Cragg MS. OX40: Structure and function — what questions remain? *Molec Immunol*. 2017;83:13—22.
71. Alam IS, Mayer AT, Sagiv-Barfi I, et al. Imaging activated T cells predicts response to cancer vaccines. *J Clin Invest*. 2018;128:2569—2580.
72. Motzer RJ, Tannir NM, McDermott DF, et al. Nivolumab plus ipilimumab versus sunitinib in advanced renal-cell carcinoma. *N Engl J Med*. 2018;378:1277—1290.
73. Hodi FS, O'Day SJ, McDermott DF, et al. Improved survival with ipilimumab in patients with metastatic melanoma. *N Engl J Med*. 2010;363:711—723.
74. Walker LS, Sansom DM. The emerging role of CTLA4 as a cell-extrinsic regulator of T cell responses. *Nat Rev Immunol*. 2011;11:852—863.
75. Higashikawa K, Yagi K, Watanabe K, et al. 64Cu-DOTA-anti-CTLA-4 mAb enabled PET visualization of CTLA-4 on the T-cell infiltrating tumor tissues. *PloS One*. 2014;9:e109866.
76. Ehlerding EB, England CG, Majewski RL, et al. ImmunoPET imaging of CTLA-4 expression in mouse models of non-small cell lung cancer. *Molec Pharmaceut*. 2017;14:1782—1789.
77. Ehlerding EB, Lee HJ, Jiang D, et al. Antibody and fragment-based PET imaging of CTLA-4+ T-cells in humanized mouse models. *Am J Cancer Res*. 2019;9:53—63.
78. Ingram JR, Blomberg OS, Rashidian M, et al. Anti-CTLA-4 therapy requires an Fc domain for efficacy. *Proc Natl Acad Sci U S A*. 2018;115:3912—3917.
79. Brochez L, Chevolet I, Kruse V. The rationale of indoleamine 2,3-dioxygenase inhibition for cancer therapy. *Eur J Cancer*. 2017;76:167—182.
80. Brandacher G, Perathoner A, Ladurner R, et al. Prognostic value of indoleamine 2,3-dioxygenase expression in colorectal cancer: effect on tumor-infiltrating T cells. *Clin Cancer Res*. 2006;12:1144—1151.
81. Okamoto A, Nikaido T, Ochiai K, et al. Indoleamine 2,3-dioxygenase serves as a marker of poor prognosis in gene expression profiles of serous ovarian cancer cells. *Clin Cancer Res*. 2005;11:6030—6039.
82. Huang X, Pan Z, Doligalski ML, et al. Evaluation of radiofluorinated carboximidamides as potential IDO-targeted PET tracers for cancer imaging. *Oncotarget*. 2017;8:46900—46914.
83. Ohta A. A metabolic immune checkpoint: adenosine in tumor microenvironment. *Front Immunol*. 2016;7:109.
84. Vijayan D, Young A, Teng MWL, Smyth MJ. Targeting immunosuppressive adenosine in cancer. *Nat Rev Cancer*. 2017;17:765.
85. Willingham SB, Ho PY, Hotson A, et al. A2AR antagonism with CPI-444 induces antitumor responses and augments efficacy to anti-PD-(L)1 and anti-CTLA-4 in preclinical models. *Cancer Immunol Res*. 2018;6:1136—1149.
86. Cekic C, Day YJ, Sag D, Linden J. Myeloid expression of adenosine A2A receptor suppresses T and NK cell responses in the solid tumor microenvironment. *Cancer Res*. 2014;74:7250—7259.
87. Barret O, Hannestad J, Vala C, et al. Characterization in humans of 18F-MNI-444, a PET radiotracer for brain adenosine 2A receptors. *J Nucl Med*. 2015;56:586—591.
88. Sakata M, Ishibashi K, Imai M, et al. Initial evaluation of an adenosine A2A receptor ligand, (11)C-preladenant, in healthy human subjects. *J Nucl Med*. 2017;58:1464—1470.

89. Goldberg MV, Drake CG. LAG-3 in cancer immunotherapy. *Curr Topics Microbiol Immunol*. 2011;344:269—278.
90. Du W, Yang M, Turner A, et al. TIM-3 as a target for cancer immunotherapy and mechanisms of action. *Int J Molec Sci*. 2017;18:E645.
91. Avogadri F, Yuan J, Yang A, Schaer D, Wolchok JD. Modulation of CTLA-4 and GITR for cancer immunotherapy. *Curr Topics Microbiol Immunol*. 2011;344:211—244.
92. Solomon BL, Garrido-Laguna I. TIGIT: a novel immunotherapy target moving from bench to bedside. *Cancer Immunol Immunother*. 2018;67:1659—1667.
93. Whelan S, Ophir E, Kotturi MF, et al. PVRIG and PVRL2 are induced in cancer and inhibit CD8(+) T-cell function. *Cancer Immunol Res*. 2019;7:257—268.
94. Malaer JD, Mathew PA. CS1 (SLAMF7, CD319) is an effective immunotherapeutic target for multiple myeloma. *Am J Cancer Res*. 2017;7:1637—1641.
95. Lines JL, Sempere LF, Broughton T, Wang L, Noelle R. VISTA is a novel broad-spectrum negative checkpoint regulator for cancer immunotherapy. *Cancer Immunol Res*. 2014;2:510—517.
96. Killock D. Immunotherapy: targeting MDSCs with LXR agonists. *Nat Rev Clin Oncol*. 2018;15:200—201.
97. Chester C, Ambulkar S, Kohrt HE. 4-1BB agonism: adding the accelerator to cancer immunotherapy. *Cancer Immunol Immunother*. 2016;65:1243—1248.
98. Jadvar H, Colletti PM. Competitive advantage of PET/MRI. *Eur J Radiol*. 2014;83:84—94.
99. Davies G, Rolle AM, Maurer A, et al. Towards translational immuno-PET/MR imaging of invasive pulmonary aspergillosis: the humanised monoclonal antibody JF5 detects aspergillus lung infections in vivo. *Theranostics*. 2017;7:3398—3414.
100. Rolle AM, Hasenberg M, Thornton CR, et al. ImmunoPET/MR imaging allows specific detection of Aspergillus fumigatus lung infection in vivo. *Proc Natl Acad Sci U S A*. 2016;113:E1026—E1033.
101. Ehman EC, Johnson GB, Villanueva-Meyer JE, et al. PET/MRI: where might it replace PET/CT? *J Magn Reson Imaging*. 2017;46:1247—1262.
102. Rhee H, Thomas P, Shepherd B, et al. Prostate specific membrane antigen positron emission tomography may improve the diagnostic accuracy of multiparametric magnetic resonance imaging in localized prostate cancer. *J Urol*. 2016;196:1261—1267.
103. Zamboglou C, Wieser G, Hennies S, et al. MRI versus (6)(8)Ga-PSMA PET/CT for gross tumour volume delineation in radiation treatment planning of primary prostate cancer. *Eur J Nucl Med Molec Imaging*. 2016;43:889—897.
104. Aerts HJ, Grossmann P, Tan Y, et al. Defining a radiomic response phenotype: a pilot study using targeted therapy in NSCLC. *Sci Rep*. 2016;6:33860.
105. Sun R, Limkin EJ, Vakalopoulou M, et al. A radiomics approach to assess tumour-infiltrating CD8 cells and response to anti-PD-1 or anti-PD-L1 immunotherapy: an imaging biomarker, retrospective multicohort study. *Lancet Oncol*. 2018;19:1180—1191.
106. Bi WL, Hosny A, Schabath MB, et al. Artificial intelligence in cancer imaging: clinical challenges and applications. *CA Cancer J Clin*. 2019;69:127—157.